



Kent Academic Repository

Rosa, Caroline Antunes, Bergantini, Alexandre, da Silveira, Enio Frota, Emilio, Marcelo, Andrade, Laerte, Pacheco, Eduardo Janot, Mason, Nigel J. and Lage, Claudia (2024) *A laboratory infrared model of astrophysical pyrimidines*. *Monthly Notices of the Royal Astronomical Society* . pp. 4794-4804. ISSN 0035-8711.

Downloaded from

<https://kar.kent.ac.uk/106323/> The University of Kent's Academic Repository KAR

The version of record is available from

<https://doi.org/10.1093/mnras/stae1457>

This document version

Publisher pdf

DOI for this version

Licence for this version

CC BY (Attribution)

Additional information

Versions of research works

Versions of Record

If this version is the version of record, it is the same as the published version available on the publisher's web site. Cite as the published version.

Author Accepted Manuscripts

If this document is identified as the Author Accepted Manuscript it is the version after peer review but before type setting, copy editing or publisher branding. Cite as Surname, Initial. (Year) 'Title of article'. To be published in **Title of Journal** , Volume and issue numbers [peer-reviewed accepted version]. Available at: DOI or URL (Accessed: date).

Enquiries

If you have questions about this document contact ResearchSupport@kent.ac.uk. Please include the URL of the record in KAR. If you believe that your, or a third party's rights have been compromised through this document please see our [Take Down policy](https://www.kent.ac.uk/guides/kar-the-kent-academic-repository#policies) (available from <https://www.kent.ac.uk/guides/kar-the-kent-academic-repository#policies>).

A laboratory infrared model of astrophysical pyrimidines

Caroline Antunes Rosa ¹★, Alexandre Bergantini ², Enio Frota da Silveira ³, Marcelo Emilio ⁴,
Laerte Andrade ⁵, Eduardo Janot Pacheco ⁶, Nigel J. Mason ^{7,8} and Claudia Lage ¹★

¹*Instituto de Biofísica Carlos Chagas Filho, Universidade Federal do Rio de Janeiro, Av. Carlos Chagas Filho, 373 - Cidade Universitária da Universidade Federal do Rio de Janeiro, CEP - 21941-170, Rio de Janeiro, RJ, Brazil*

²*Centro Federal de Educação Tecnológica Celso Suckow da Fonseca, Av. Maracanã 229, CEP - 20271-110, Rio de Janeiro, RJ, Brazil*

³*Departamento de Física, Pontifícia Universidade Católica do Rio de Janeiro, Rua Marquês de São Vicente 225, CEP - 22451-900, Rio de Janeiro, RJ, Brazil*

⁴*Departamento de Geociências, Universidade Estadual de Ponta Grossa, Av. General Carlos Cavalcanti, 4748, CEP - 84030-900, Ponta Grossa, PR, Brazil*

⁵*Laboratório Nacional de Astrofísica, R. dos Estados Unidos, 154, CEP - 37504-364, Itajubá, MG, Brazil*

⁶*Instituto de Astronomia, Geofísica e Ciências Atmosféricas - IAG, Universidade de São Paulo, R. do Matão, 1226, CEP - 05508-090, São Paulo, SP, Brazil*

⁷*Centre for Astrophysics and Planetary Science, School of Physics and Astronomy, University of Kent, Canterbury CT2 7NH, UK*

⁸*Atomic and Molecular Physics Laboratory, Atomki Institute for Nuclear Research, Debrecen H-4026, Hungary*

Accepted 2024 June 5. Received 2024 June 3; in original form 2023 August 16

ABSTRACT

Nucleobases are essential molecules for life, forming integral parts of deoxyribonucleic acid (DNA) and ribonucleic acid (RNA) in all terrestrial life forms. Despite evidence of their abiotic synthesis in meteorites and laboratory simulations of interstellar medium (ISM) conditions, nucleobases have not been detected in the ISM. This study investigates the infrared spectra of uracil, cytosine, and thymine – pyrimidine nucleobases – embedded in an ice mixture simulating common volatiles found in protostellar discs. Our objective was to explore the feasibility of identifying unique infrared bands of pyrimidines in the ISM, despite significant overlapping absorption features from simpler, more abundant interstellar species such as H₂O, CO, CH₃OH, and NH₃. Laboratory results revealed that although two common bands (1240 and 760 cm⁻¹ in uracil; 1236 and 763 cm⁻¹ in cytosine; and 1249 and 760 cm⁻¹ in thymine) were identified, the detection of these bands in space is challenged by overlapping absorption features. Recent observations with the *JWST* have shown that interstellar organic species exhibit infrared signals within similar ranges, making it impossible to distinguish pyrimidine bands from these organics. Thus, detecting pyrimidines with current telescopes is infeasible, not due to sensitivity limitations or the need for more powerful instrumentation, but because of the intrinsic overlap in spectral features. This study complements previous research on purines by examining pyrimidines and including the impact of common ISM volatiles in the ice composition. The results highlight the significant challenges in detecting complex molecules in the ISM, underscoring the importance of understanding the spectral complexities and interactions to interpret astronomical observations accurately.

Key words: Astrochemistry – methods: laboratory: solid state – ISM: molecules – infrared: general.

1 INTRODUCTION

Nucleobases are essential molecules for life as we know it. They are key molecules in evolutionary, genetic, and hereditary processes in all life forms on Earth, being the aromatic nitrogen heterocyclic (N-heterocycles) chemical species present in DNA and RNA. There are two groups of nucleobases: (i) purines, which are formed by the fusion of two rings – a pyrimidine ring and an imidazole ring, and (ii) pyrimidines, which are made of a pyrimidine ring only. For life on Earth, the purines present in nucleic acids are adenine (C₅H₅N₅) and guanine (C₅H₅N₅O), the pyrimidines present in nucleic acids of living organisms are cytosine (C₄H₅N₃O – DNA and RNA), thymine (C₅H₆N₂O₂ – DNA only), and uracil (C₄H₄N₂O₂ – RNA only). However, it is worth mentioning that there are other

purines and pyrimidines in nature, besides the ones present in nucleic acids, which may or may not participate in biological functions. Nucleobases from each group are differentiated by the functional groups hanging off the ring (Fig. 1).

How complex molecules such as nucleobases were formed and incorporated into the first living organisms on Earth remains a matter of debate (Saladino et al. 2012). Early hypothesis suggested that the building blocks of life were formed via chemical reactions between simple molecules present in the early Earth's atmosphere and oceans (Kobayashi 2019). Indeed, a series of experiments have demonstrated that nucleobases can be formed in conditions analogue to those found in primitive Earth (Kitadai & Maruyama 2018). It is known that pyrimidines can be abiotically synthesized. For example, uracil and cytosine can be synthesized from cyanoacetylene (C₃HN) (Fox & Harada 1961, Ferris et al. 1968) – a chemical species which has been detected in the interstellar medium (ISM, Turner 1971). According to Choughuley et al. (1977) and Schwartz & Chittenden

* E-mail: cantunesbio@gmail.com (CAR); lage@biof.ufjf.br (CL)

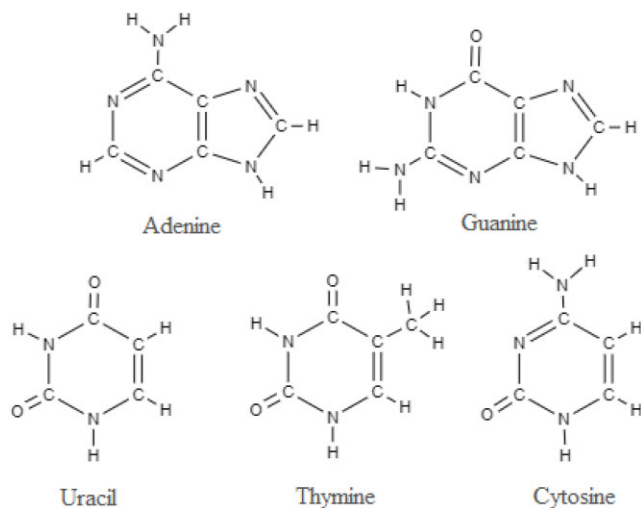


Figure 1. Nucleobases found in nucleic acids on Earth.

(1977), thymine can be formed from reactions between uracil and formaldehyde (CH_2O , a species found in the ISM as well). Among the several experiments reporting the abiotic synthesis of nucleobases, the ones that seem to yield the most promising results use formamide (NH_2CHO , detected in the ISM by Rubin et al. 1971) as the main precursor. Indeed, it has been shown that it is possible to synthesize all nucleobases found both in DNA and RNA from the polymerization of formamide under high temperature in early-Earth-like scenarios (Saladino et al. 2001, 2003, 2004, 2006, 2012).

Besides experimental evidence for routes of terrestrial abiotic synthesis of nucleobases, an alternative hypothesis suggests that the ingredients for early-life forms were produced on dust grain mantles found in cold and dense gas envelopes in the protostellar stage and delivered to Earth by meteorites and comets that collided with the planet, mainly during the ‘late heavy bombardment’ epoch, about 4 billion years ago (Chyba & Sagan 1992, Sandford et al. 2020). This hypothesis is supported by the observation of an extensive number of biomolecules, such as amino acids, nucleobases, sugars, and aliphatic molecules (bio-membrane precursors) found in meteorites (Hayatsu et al. 1975, Stoks & Schwartz 1979, Deamer & Pashley 1989, Shock & Schulte 1990, Cooper et al. 2001, Sephton 2002, Martins et al. 2008, Callahan et al. 2011, Burton et al. 2012, Cooper & Rios 2016, Furukawa et al. 2019). Calculations made by Chyba and Sagan (1992) suggested that the amount of organic material produced on Earth (i.e. endogenous material) and delivered from outside Earth (i.e. exogenous material) may have contributed equally to the origin of life in the planet.

In a recent study, Oba et al. (2022), using new analytical techniques, reported the detection of all terrestrial life nucleobases – adenine, guanine, thymine, cytosine, and uracil – in the fragments of the meteorites *Murray*, *Tagish Lake*, and *Murchison*. Furthermore, laboratory experiments simulating ISM conditions have demonstrated that the synthesis of nucleobases on the surface of ices under electromagnetic and/or ion irradiation is plausible (Saladino et al. 2005, Nuevo & Sandford 2014, Materese et al. 2018, Oba et al. 2019, Ruf et al. 2019). For example, from the ultraviolet (UV, Lyman- α) irradiation of purine ($\text{C}_5\text{H}_4\text{N}_4$) and pyrimidine ($\text{C}_4\text{H}_4\text{N}_2$) with different mixtures of commonly found ISM species (including H_2O , CH_3OH , NH_3 and CH_4), the synthesis of adenine, guanine, uracil, cytosine, and thymine was obtained (Nuevo et al. 2009, 2012; Materese et al. 2013, 2017). Oba et al. (2019) also performed an

experiment with an interstellar ice analogue containing a mixture of $\text{H}_2\text{O}:\text{CO}:\text{CH}_3\text{OH}:\text{NH}_3$ (5:2:2:2) irradiated with UV (Lyman- α) at 10 K in ultrahigh vacuum. They were able to produce cytosine, uracil, thymine, adenine, hypoxanthine, xanthine, and nitrogen heterocycles. Ruf et al. (2019) also demonstrated the synthesis of cytosine from an ice mixture containing $\text{H}_2\text{O}:\text{CH}_3\text{OH}:\text{NH}_3$ (2:1:1) irradiated with Lyman- α in a simulated astrophysical environment. Both experiments demonstrated that nucleobases could be formed from non-cyclic molecules in realistic ISM conditions. Indeed, the simple molecular species used in these experiments are abundant in protostellar discs (Öberg et al. 2011), making these regions favourable for the synthesis of biomolecules (Bergantini et al. 2017).

From an astronomical point of view, nucleobases are labelled as complex organic molecules (COMs) since they contain more than six atoms (Herbst & Van Dishoeck 2009) and the nitrogen incorporated to the ring increases the complexity of the astrophysical synthesis of these molecules (Parker et al. 2015). According to Sandford et al. (2020) and Dullemond et al. (2020), the region known as the mid-plane of the middle of the protostellar disc can reach temperatures lower than 20 K and COMs are believed to be produced on the dust grain mantles in these discs (Danger et al. 2011, Maity et al. 2015, Öberg 2016). Due to temperature increase and/or shocks associated with accretion and outflow activities (among other phenomena) around protostellar discs, the COMs produced in the solid phase can be liberated from the dust grains (Zhang et al. 2023), thus going to gas phase. Thanks to the Atacama Large Millimeter/submillimeter Array and other large radio facilities (e.g. Institute for Radio Astronomy in the Millimetre Range - IRAM 30 m) COMs and many organic molecules are being observed in several of these objects (e.g. Baek et al. 2022; Coutens et al. 2022; Guélin & Cernicharo 2022). However, no purine or pyrimidine has been identified, in either phase, towards objects of the ISM so far, including attempts made by Simon & Simon (1973), Charnley et al. (2005), and Brünken et al. (2006). Identifying complex molecules in the ISM is a major challenge, since the larger the molecule, the more complex is its spectral signature. It is especially difficult to detect species which are in low concentration, since many of the distinctive spectral features (i.e. their ‘fingerprint’) may be concealed by bands of higher concentration species (Janot-Pacheco et al. 2018).

However, the detection of pyrimidines or other complex molecules in the solid phase toward ISM objects is highly challenging if not impossible. This is due to the significant overlap of their infrared (IR) bands with those of many other molecules that have similar functional groups. Specifically, the C–H and C–O absorption features of various possible molecules contribute at 7.8 μm , and ice features are present in the range between 6.8 and 8.5 μm . Additionally, molecules such as CH_4 , SO_2 , HCOOH , CH_3CHO , and $\text{CH}_3\text{CH}_2\text{OH}$ are expected to absorb in the targeted wavelength range. The absorption profiles of H_2O and CH_3OH around 6.8 μm from ice mixtures, along with the shared band at 7.2 μm between HCOO^- and HCOOH , further complicate the detection. Therefore, even with more powerful instrumentation, the overlapping absorption features make it impossible to distinctly determine the characteristic IR bands of pyrimidines or other complex molecules.

Therefore, in this study, the IR spectra of a mixture of molecules, at cryogenic temperatures, containing $\text{H}_2\text{O}:\text{CO}:\text{CH}_3\text{OH}:\text{NH}_3$ deposited on top of uracil, cytosine, and thymine, were collected, as these volatiles are potential precursors of interstellar nucleobases (Nuevo & Sandford 2014, Materese et al. 2018, Oba et al. 2019, Ruf et al. 2019). Data were collected both at room (300 K) and cryogenic temperatures (15 K). Room-temperature spectra are compatible with the later stages and inner portions of the protostellar disc,

where the temperatures can easily reach 300 K and more (Boss 1998). Conversely, the outer regions, as well as the midplane of the middle of the protostellar disc, are found in temperatures ranging from 10 to 100 K (Sandford et al. 2020). Our main objective is to explore the feasibility of identifying any unique IR bands of pyrimidines related to nucleobases in the ISM, despite the presence of overlapping absorption features from common ISM species (i.e. $\text{H}_2\text{O}:\text{CO}:\text{CH}_3\text{OH}:\text{NH}_3$). This study complements a previous study on purines which proposed their interstellar IR spectral signature (Rosa et al. 2023). Although distinct identification may be impossible, understanding the spectral complexities and interactions provides valuable insights for interpreting astronomical observations and the chemical composition of the ISM.

2 METHODOLOGY

2.1 Experimental apparatus

The experiments were performed at the Van de Graaff Laboratory of the Pontifical Catholic University of Rio de Janeiro (PUC-Rio). The experimental apparatus consists of a high-vacuum chamber, a Fourier transform infrared spectrometer (FTIR – Jasco FT-IR-4200), a sample holder which can be cooled down to 15 K using a closed-cycle helium cryostat (CCS-UHV/204 Janis Research Company cold head and Sumitomo HC-4E compressor). The base pressure of the chamber during the experiments was of the order of 10^{-8} mbar. The nucleobases cytosine, thymine, and uracil (≥ 99 per cent purity) in powder form were purchased from Sigma–Aldrich. The powdered pyrimidines were deposited onto ZnSe substrates as a thin film produced by sublimation inside a separated high-vacuum chamber (Edwards E306 model). The thickness of each pyrimidine sample was measured *in situ* by a quartz crystal microbalance. After producing the pyrimidine thin film, the sample was then transferred to the main experimental high-vacuum chamber, which was then pumped down for 12–24 h, after which the substrate was cooled down to approximately 15 K. Then, a $\text{H}_2\text{O}:\text{CO}:\text{CH}_3\text{OH}:\text{NH}_3$ gas mixture (prepared in a separated chamber) was deposited on top of the pyrimidine film. Since the pyrimidines of interest are solid at room temperature, we have used the methodology described by Saïagh et al. (2014) to prepare our samples, which consisted of a condensed layer of gases on top of a previously evaporated layer of nucleobase. The final result is a sample made of two main layers: the bottom layer is the nucleobase, and the top layer is the gas mixture. The gas mixture was prepared as follows: the gases were added one at a time in a separated gas-mixing chamber (GMC). First, 16 mbar of a 2:1 solution of H_2O and CH_3OH was added. Then, 4 mbar of CO and 4 mbar of NH_3 were added, respectively, resulting in the final total pressure of 24 mbar. The GMC was otherwise kept at 10^{-6} mbar to avoid contamination. The 2:1 solution of H_2O and CH_3OH was determined empirically to produce the final desired ratio of 5:2 in ice form.

Once the mixture was prepared, a leak valve was used to let the gas mixture into the main experimental chamber. During the mixture deposition, the main chamber pressure was kept at $(5 \pm 3) \times 10^{-7}$ mbar. Each mixture deposition lasted for approximately 10 min. The chemical composition of the sample was analysed online and *in situ* immediately after deposition using FTIR spectroscopy.

IR spectra (120 scans per spectrum at 4 cm^{-1} of resolution) in the 4500 to 650 cm^{-1} range (~ 2 to $15 \mu\text{m}$) were collected in each of the following steps: (i) when the substrate containing the evaporated pyrimidine nucleobase was loaded in the experimental chamber at room pressure and temperature; (ii) when the pressure of the chamber

was evacuated to $\sim 10^{-8}$ mbar (high vacuum) at room temperature; and (iii) in high vacuum and at 15 K, before and after the deposition of the gas mixture.

2.2 Column density calculation

The column densities (N) and the ratios between the ices and the pyrimidine nucleobases were calculated using a modified Lambert–Beer equation (1) (Bergantini et al. 2018):

$$N = \ln 10 \frac{\int_{\nu_1}^{\nu_2} ||d\nu||}{A \text{ value}}, \quad (1)$$

where $\int_{\nu_1}^{\nu_2} ||d\nu||$ is the integrated peak area the IR band of interest, and the A value is the IR absorption coefficient (also called band strength). The A values of the water, methanol, ammonia, and carbon monoxide bands used in the calculations were extracted from Bouilloud et al. (2015). The pyrimidines column densities were measured as follows: the A value used for the uracil sample was the one from the β band, which is defined as the integrated band strength of the bands found between 3400 to 1890 cm^{-1} of uracil (Saïagh et al. 2015). Similarly for cytosine, the A value used was the α band, which is defined as integrated band strength between 3500 to 2000 cm^{-1} of the cytosine spectrum (Vignoli Muniz et al. 2022). To characterize thymine the 940 cm^{-1} band was used (Mejía et al. 2023). These considerations resulted in the following ratio calculated from the column densities: $10:5:0.2:19:5$ ($\text{H}_2\text{O}:\text{CO}:\text{NH}_3:\text{CH}_3\text{OH}:\text{Uracil}$), $10:3:2:8:0.7$ ($\text{H}_2\text{O}:\text{CO}:\text{NH}_3:\text{CH}_3\text{OH}:\text{Cytosine}$), and $10:0.8:0.1:3:0.3$ ($\text{H}_2\text{O}:\text{CO}:\text{NH}_3:\text{CH}_3\text{OH}:\text{Thymine}$).

3 RESULTS

3.1 The infrared signatures of the pyrimidines uracil, cytosine, and thymine

The crystalline IR spectra of the neat uracil, cytosine, and thymine obtained at 300 and 15 K are presented in Figs 2 and 3, respectively. The crystallinity of the samples was verified by comparison with data from the literature (Szczeniak et al. 1985). The assignments of the observed IR bands are shown in Table 1. The observed bands were characterized according to the literature (Susi & Ard 1971; Radchenko et al. 1984; Mathlouthi et al. 1986; Szczeniak et al. 1988, 2000; Nowak et al. 1989; Leś et al. 1992; Kwiatkowski & Leszczyński 1996; Colarusso et al. 1997; Singh 2008; Fornaro et al. 2014; Saïagh et al. 2015).

The spectral region between ~ 3360 and $\sim 2650 \text{ cm}^{-1}$ is characterized by C-H and N-H out of the ring stretching vibration modes for all three of the pyrimidines analysed, in addition to the stretching modes of the functional groups attached to the ring, such as the cytosine’s amino group and the thymine’s methyl group. The region between ~ 1780 and 650 cm^{-1} is characterized by $\nu\text{C-C}$, $\nu\text{C-N}$, $\nu\text{C} = \text{C}$, $\nu\text{C} = \text{N}$, and $\nu\text{C} = \text{O}$ modes as well as by the bending modes out of the rings’ functional groups. In this region, the vibration modes of the whole molecule, such as the β Ring, the ν Ring, and the ring-breathing modes, are also observed. There are similarities between the spectra of uracil, cytosine, and thymine since all these species belong to the pyrimidines group. Some bands are found near the same position in all the three pyrimidines’ spectra. There are six such bands with similar wavenumbers: uracil’s 1674, 1462, 1240, 1012, 806, and 760 cm^{-1} bands; cytosine’s 1661, 1467, 1236, 1013, 795, and 763 cm^{-1} bands; and thymine’s 1673, 1459, 1249, 1027, 816, and 760 cm^{-1} bands. For all three pyrimidines, the $\sim 760 \text{ cm}^{-1}$ band is attributed

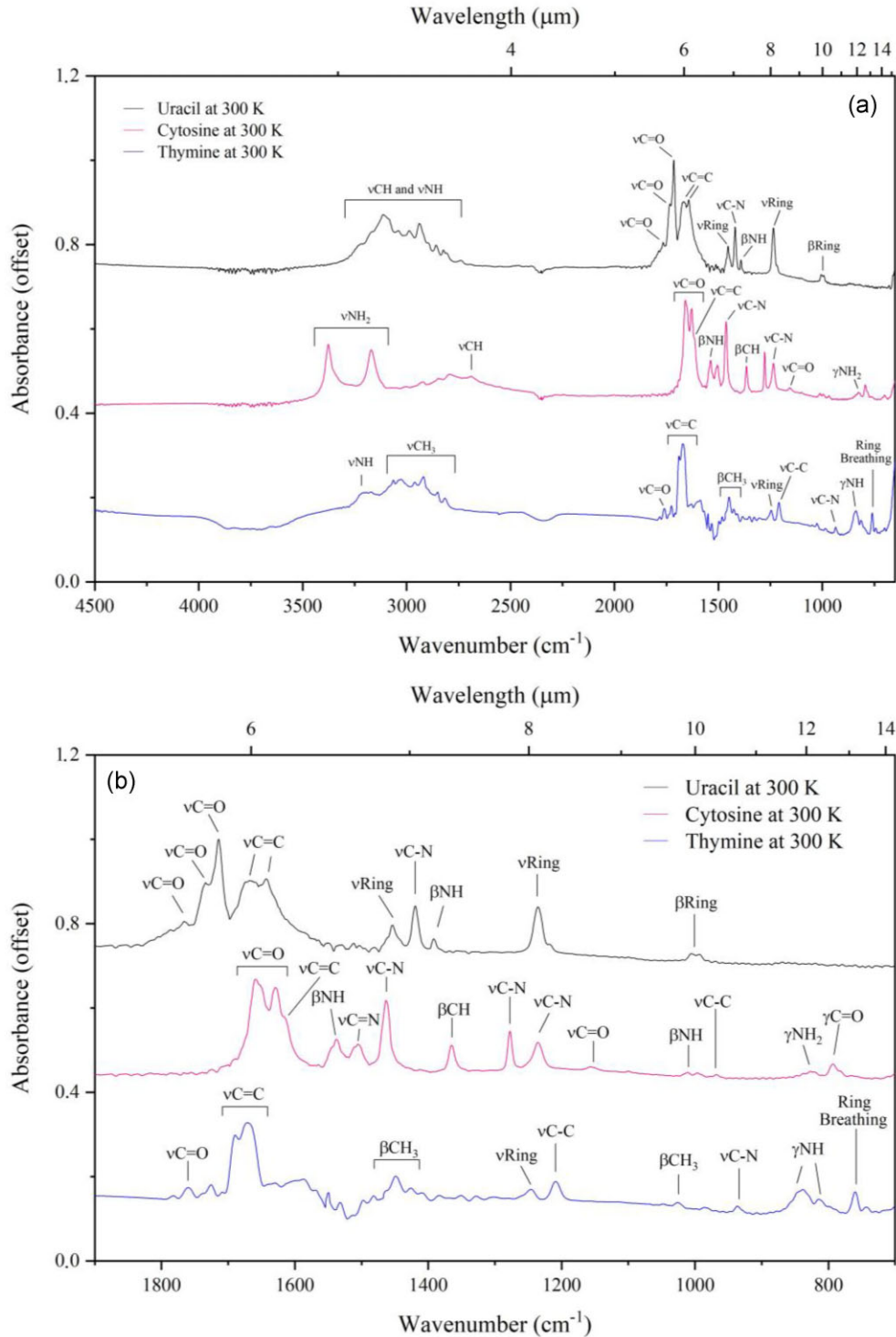


Figure 2. (a) Mid-IR spectra of uracil (upper line), cytosine (middle line), and thymine (bottom line) at 300 K, in high vacuum. The main bands are identified by their assignments. (b) The fingerprint region ($1900\text{--}700\text{ cm}^{-1}$) of pyrimidines uracil (upper line), cytosine (middle line), and thymine (bottom line). The top scale is in wavelength (μm), while the bottom scale is in wavenumber (cm^{-1}), a common unit used in laboratory IR spectroscopy. Abbreviations: ν – stretching; β – in plane bending; γ – out of plane bending; and δ – scissoring.

to the ring-breathing mode, a characteristic vibration for the whole ring. For this reason, this band could be used as a signature of the three pyrimidines present in DNA and RNA.

To understand how the IR bands of uracil, cytosine, and/or thymine contribute to the observed spectra in cold clouds and

protostellar discs, it is necessary to take into account the chemical environment within which the molecules are found. According to recent experimental and theoretical studies (e.g. Bergantini et al. 2017; Vasyunin et al. 2017; Bergantini et al. 2018; Ioppolo et al. 2021), the interstellar synthesis of COMs, which potentially includes

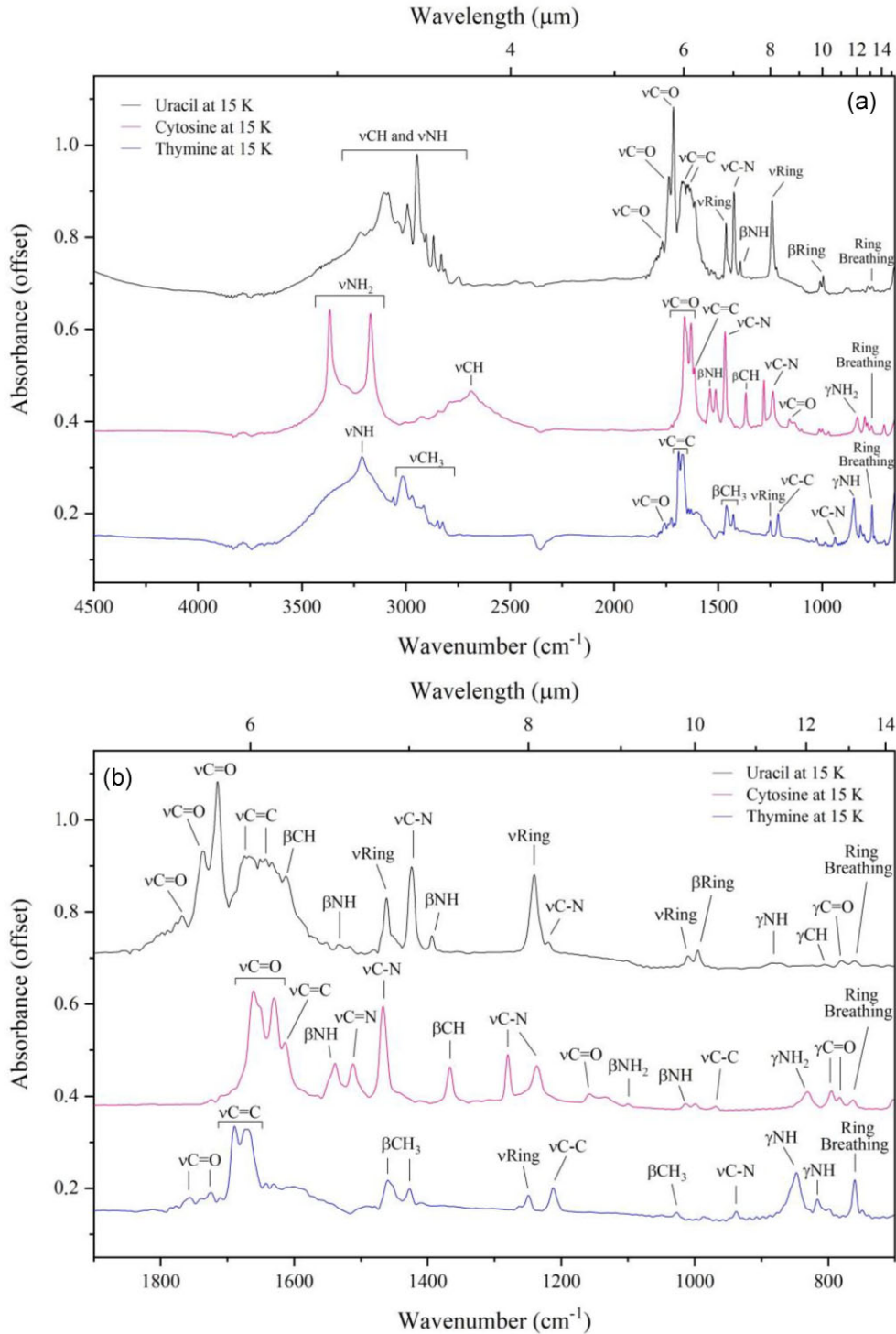


Figure 3. (a) Mid-IR spectra of uracil (upper line), cytosine (middle line), and thymine (bottom line) at 15 K, in high vacuum. The main bands are identified by their assignments. (b) The fingerprint region (1900–700 cm⁻¹) of pyrimidines uracil (upper line), cytosine (middle line), and thymine (bottom line). The top scale is in wavelength (μm), while the bottom scale is in wavenumber (cm⁻¹), a common unit used in laboratory IR spectroscopy. Abbreviations: ν – stretching; β – in plane bending; γ – out of plane bending; and δ – scissoring.

pyrimidines, is likely to occur in gas and dust-enriched cold regions, via non-thermal, energetic, and non-energetic mechanisms. These conditions are mainly found in the outer regions, as well as the mid-plane of the middle of the protostellar discs. Therefore, the IR spectra of uracil, cytosine, and thymine was collected embedded in a

realistic interstellar ice analogue, which contained some of the most abundant species found in polar ices found within protostellar discs (Öberg et al. 2011; Boogert et al. 2015; McClure et al. 2023). Our aim was to determine if, and how, the spectrum of uracil, cytosine, and thymine would change when common molecular species, such

Table 1. Assignment of the IR bands observed in uracil, cytosine, and thymine's spectra at 300 and 15 K.

Uracil		Cytosine		Thymine	
300 K	15 K	300 K	15 K	300 K	15 K
ν (cm ⁻¹)	ν (cm ⁻¹)	ν (cm ⁻¹)	ν (cm ⁻¹)	ν (cm ⁻¹)	ν (cm ⁻¹)
Assignment	Assignment	Assignment	Assignment	Assignment	Assignment
3112	3107	3376	3366	3205	3211
ν C-H; ν N-H	ν C-H; ν N-H	$\nu_{\text{asym}}\text{NH}_2$	$\nu_{\text{asym}}\text{NH}_2$	ν N-H	ν N-H
3087	3085	3170	3171	3063	3062
		$\nu_{\text{sym}}\text{NH}_2$	$\nu_{\text{sym}}\text{NH}_2$	ν C-H	ν C-H
2988	2993	2692	2688	3026	3016
		ν C-H	ν C-H	$\nu_{\text{asym}}\text{CH}_3$	$\nu_{\text{asym}}\text{CH}_3$
2938	2948	1659	1661	2963	2972
		ν C=O	ν C=O	ν CH ₃	ν CH ₃
2898	2903	1629	1630	2919	2918
		ν C=C	ν C=C	ν CH ₃	ν CH ₃
2858	2868	1616	1614	2851	2848
		β N-H	β N-H	ν C=O	ν C=O
2823	2831	1538	1539	1760	1756
		ν C=O	ν C=O	ν C=O	ν C=O
1768	1768	1505	1512	1726	1725
		ν C=O	ν C=O	ν C=O	ν C=O
1735	1736	1463	1467	1689	1689
		ν C=O	ν C-H	ν C=C	ν C=C
1714	1715	1365	1366	1671	1673
		ν C=C	β C-H	ν C=C	ν C=C
1667	1674	1278	1280	1449	1459
		ν C=C	ν C-N	β CH ₃	β CH ₃
1643	1643	1235	1236	1426	1427
		ν C=C	ν C-N	β CH ₃	β CH ₃
-	1616	1157	1158	1246	1249
	β C-H	ν C=O	ν C=O	ν Ring	ν Ring
1533	1535	1100	1099	1209	1212
	β N-H	β N-H	$\beta_{\text{rock}}\text{NH}_2$	β C-H, ν C-N, ν C-C, ν C-CH ₃	β C-H, ν C-N, ν C-C, ν C-CH ₃
1454	1462	1011	1013	1026	1027
	ν Ring, ν C-N and β N-H	ν C-N and β C-H	β N-H and β C-H	$\beta_{\text{rock}}\text{CH}_3$ and ν Ring	$\beta_{\text{rock}}\text{CH}_3$ and ν Ring
1419	1424	998	999	936	938
	ν C-N and β N-H	ν C-H	ν C-H	ν C-N	ν C-N
1392	1394	969	969	838	847
	β N-H; β C-H and ν C-N	ν C-C	ν C-C	γ N-H	γ N-H
1235	1240	827	831	814	816
	ν Ring	γ NH ₂	γ NH ₂	γ N-H	γ N-H
1220	1221	793	795	760	760
	ν C-N, β N-H and β C-H	ν C=O	ν C=O	Ring breathing and ν C=O	Ring breathing and ν C=O
1005	1012	783	783	743	749
	ν Ring	β Ring	β Ring		
-	881	700	702		
	γ NH	Ring breathing	Ring breathing		
-	806	γ C-H and γ C=O			
	γ C-H and γ C=O				
-	780	γ C=O			
	γ C=O				
-	760	Ring breathing			
	Ring breathing				

Notes. Refs. 1: Colarusso et al. (1997), 2: Lesć et al. (1992), 3: Susi & Ard (1971), 4: Saigah et al. (2015), 5: Fornaro et al. (2014), 6: Mathlouthi et al. (1986), 7: Kwiatkowski & Leszczyński (1996), 8: Radchenko et al. (1984), 9: Szczesniak et al. (1988), 10: Nowak et al. (1989), 11: Singh (2008), and 12: Szczepaniak et al. (2000).

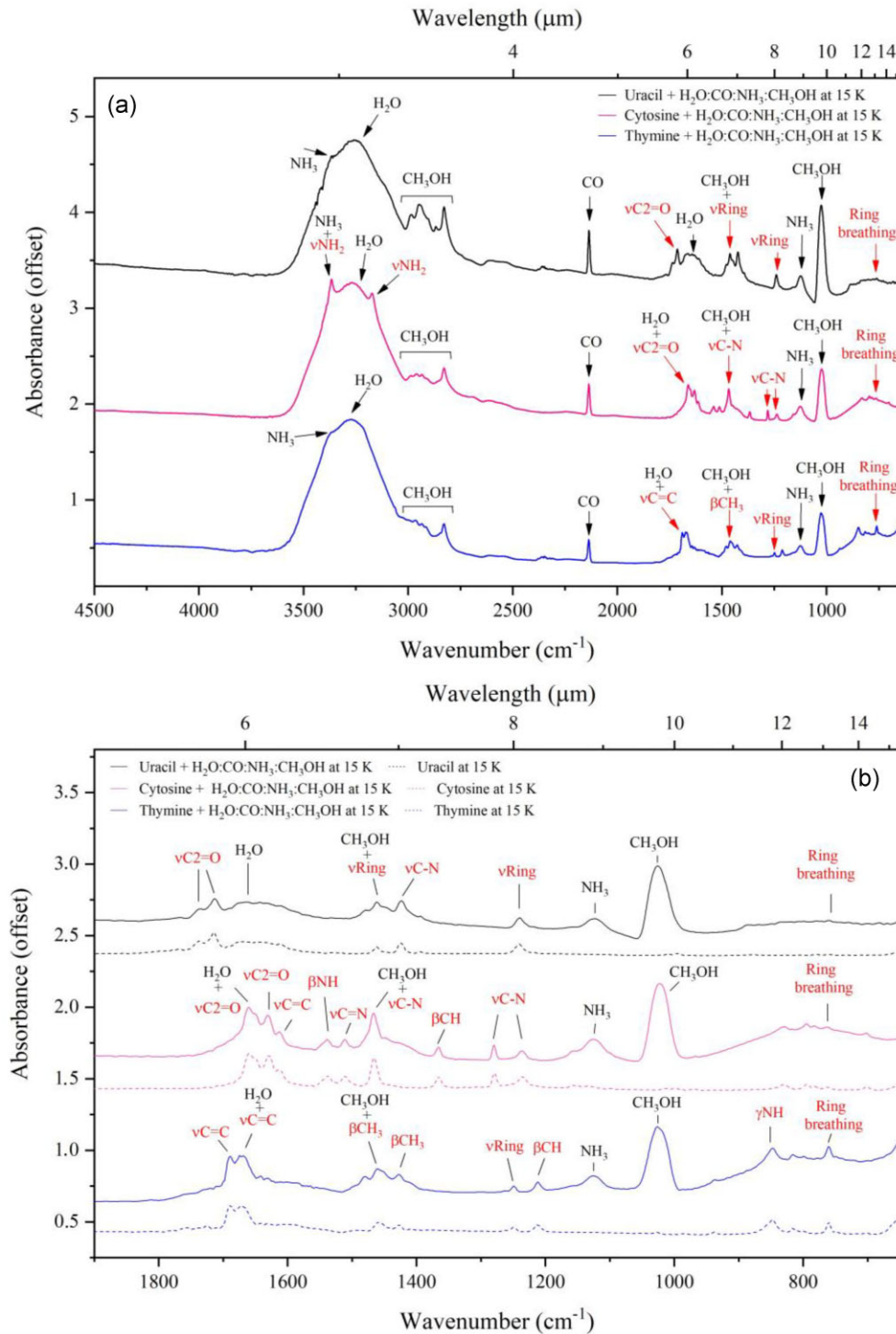


Figure 4. (a) Mid-IR spectra of uracil (upper line), cytosine (middle line), and thymine (bottom line) covered by common ISM volatiles at 15 K. (b) The fingerprint region ($1900\text{--}650\text{ cm}^{-1}$) of pyrimidines uracil (upper line), cytosine (middle line), and thymine (bottom line) is covered by common ISM volatiles at 15 K. Red (light) arrows indicate transitions assigned to the nucleobases and black arrows indicate transitions assigned to the ice mixture. Based on the column densities, the calculated mixture ratios are: H₂O:CO:NH₃:CH₃OH:Uracil (10:5:2:19:5); H₂O:CO:NH₃:CH₃OH:Cytosine (10:3:2:8:0.7); and H₂O:CO:NH₃:CH₃OH:Thymine (10:0.8:0.1:3:0.3). The top scale is in wavelength (μm), while the bottom scale is in wavenumber (cm^{-1}). Abbreviations: ν – stretching; β – in plane bending; γ – out of plane bending; and δ – scissoring.

as H₂O:CO:CH₃OH:NH₃, are condensed onto it, thus possibly mimicking the ice mantles found in the coldest regions of protostellar discs. The IR spectra of these three pyrimidines embedded in a H₂O:CO:CH₃OH:NH₃ mixture at 15 K is shown in Fig. 4. The IR

modes of uracil, cytosine and thymine are indicated by red arrows and the modes of H₂O, CO, NH₃, and CH₃OH by black arrows. The icy samples whose spectra are shown in Fig. 4 present a layered structure. Even though the reaction mechanisms that take place in

ice mixtures versus layered ices are mostly likely different from each other, for the purposes of this investigation (i.e. the characterization of IR bands of pyrimidines in space), the spectra of layered ices can be considered a valid effort to be used in astrophysical observations.

Fig. 4 shows that most IR bands of uracil, cytosine, and thymine are overlapped by the volatiles bands. As a result, even the weak lower energy transitions, which are less affected by overlapping, are not sufficiently distinguishable to be detected in future observations. This is because the overlapping absorption features from common ISM species, such as H₂O, CO, CH₃OH, and NH₃, create a complex background that masks the unique spectral signatures of the pyrimidines. The region between 3500 and 2700 cm⁻¹ is completely dominated by the strong water, ammonia, and methanol bands, and the stretching mode of CO occurs in a region without pyrimidines bands. The bending mode of water is found in the same region where one of the strongest bands of pyrimidines (~1700 cm⁻¹) is expected to be found. In the region near ~1460 cm⁻¹, the CH and OH bending modes of CH₃OH are observed. This band also overlaps some important pyrimidine bands; the same occurs in the region between ~1100 and 1000 cm⁻¹, where the umbrella mode of NH₃ and the stretching mode of CO (CH₃OH) bands overlap the signatures of the pyrimidine's nucleobases. Only a few pyrimidine bands are observed between 1600 and 650 cm⁻¹. The assignments of the IR bands observed in Fig. 4 are presented in Table 2.

Some of the pyrimidine's bands have similar wavenumbers, such as the bands 1240 cm⁻¹ (ν Ring) and 760 cm⁻¹ (Ring breathing) in uracil's spectrum, 1236 cm⁻¹ (ν C-N) and 763 cm⁻¹ (Ring breathing) in cytosine's spectrum, and 1249 cm⁻¹ (ν Ring) and 760 cm⁻¹ (Ring breathing) in thymine's spectrum (Fig. 5).

The common pyrimidines bands presented in Fig. 5 are characteristic of vibration modes of the whole ring, rendering a specific signature for the ensemble of pyrimidines. Therefore, their detection is complicated by overlap with simpler interstellar organic species, which are expected to be more abundant. For example, the vibrational transitions of CH₃OCHO (1211 cm⁻¹) and H₂CO (1244 cm⁻¹) fall within the same spectral region. Additionally, the weak ring breathing mode of thymine at 760 cm⁻¹ coincides with the absorption region of H₂O, further complicating the detection. Even if these bands are weak in intensity, if uracil, cytosine, or thymine were present altogether in the same astrophysical target, these common bands with similar wavenumbers may blend, making the spectral profile broader and/or more prominent. For this reason, the detection and identification of individual pyrimidines are challenging. The overlap of these common bands complicates the quantification of each species' contribution to the overall spectral profile.

4 CHALLENGES IN IDENTIFYING PYRIMIDINE BANDS IN INTERSTELLAR ICE SPECTRA

The IR bands discussed in this study are characterized in Table 3, which also includes the integrated molar absorptivity (ψ) for each band, as calculated by Iglesias-Groth and Cataldo (2023). Searching the interstellar ice inventory for spectroscopic features of other simple common ice species at wavelengths similar to those discussed here for pyrimidines did not yield any identifiable bands around 8.05 and 13.14 μ m, the regions of interest for pyrimidines (Gibb et al. 2004; Boogert et al. 2015; McClure et al. 2023). Recent observations made by *JWST* revealed that interstellar organic species such as CH₃OCHO, CH₃COOH, and HCOOH, which are expected to be more abundant than pyrimidines, exhibit IR signals between 7.8–8.6 μ m (Rocha et al. 2024). Therefore, even *JWST* would

not be able to distinguish the $8.05 \pm 0.08 \mu$ m band of pyrimidines from these organic compounds. Additionally, although the $13.14 \pm 0.10 \mu$ m band of pyrimidines is distinguishable from the libration mode of water (13.6 μ m) in laboratory spectra, it would be difficult to separate these bands in observations. Thus, detecting pyrimidines with current telescopes is impossible due to overlapping absorption features, not a matter of sensitivity or more powerful instrumentation.

5 CONCLUSIONS

Nucleobases are essential molecules for life since they form an integral part of the DNA and RNA present in all life forms on Earth. There is evidence for the abiotic synthesis of nucleobases outside Earth as they have been detected in meteorites (Oba et al. 2022) and laboratory experiments have revealed that they can be synthesized in ISM ices (Oba et al. 2019, Ruf et al. 2019). Despite this, nucleobases have never been detected in the ISM. It is unlikely that the solar system is the only place where such molecules are formed. Therefore, it is almost certain that the detection of nucleobases outside Earth is hindered by the challenges inherently associated with the detection methods. Laboratory studies, such as the one presented here, reveal the challenges to observe these complex molecules in outer space.

In the current paper, we present the IR spectra of uracil, cytosine, and thymine, the pyrimidines nucleobases found in DNA and in RNA, embedded in an ice mixture that represents the most common volatiles found protostellar discs. Pyrimidines IR bands can potentially lead to their identification even in environments rich in H₂O, CO, CH₃OH, and NH₃. It was possible to identify two common bands which are not covered by volatiles at 1240 and 760 cm⁻¹ in uracil's spectrum; 1236 and 763 cm⁻¹ in cytosine's spectrum, and 1249 and 760 cm⁻¹ in thymine's spectrum. However, even these bands are not proposed as definitive spectral signatures for pyrimidines in the ISM due to the complexity of distinguishing them in the presence of overlapping features.

In a previous study, our group performed a similar experiment and analysis for the purine family (Rosa et al. 2023). This study complements the previous one, not only by investigating the other family of life-related nucleobases – the pyrimidines – but also by including the effects of the presence of common ISM volatiles in the composition of the ice. While searching for common bands from each group of nucleobases (purines and pyrimidines) in astrophysical targets could potentially increase the overall signal of these low-intensity bands, the inherent challenges in detection remain significant. The low abundance of nucleobases in such environments, compared to simpler species, further complicates their detection. Thus, detecting pyrimidines with current telescopes is impossible due to overlapping absorption features, and this issue is not merely a matter of sensitivity or more powerful instrumentation.

AUTHOR CONTRIBUTION STATEMENT

Caroline Antunes Rosa: Conceptualization (Lead); Formal analysis (lead); Methodology (supporting); Software (equal); Visualization (lead); Writing – original draft (lead); Writing – review & editing (lead). Alexandre Bergantini: Methodology (lead); Software (equal); Supervision (equal); Formal analysis (supporting); Conceptualization (supporting); Writing – original draft (supporting); Writing – review and editing (supporting). Enio Frota da Silveira: Methodology (supporting); Writing – original draft (support-

Table 2. Assignment of observed bands in uracil, cytosine, and thymine spectrum covered with common ISM volatiles at 15 K and high vacuum.

Uracil + H ₂ O:CO:NH ₃ :CH ₃ OH ν (cm ⁻¹)	Assignment	Cytosine + H ₂ O:CO:NH ₃ :CH ₃ OH ν (cm ⁻¹)	Assignment	Thymine + H ₂ O:CO:NH ₃ :CH ₃ OH ν (cm ⁻¹)	Assignment
3370	ν_3 of NH ₃ (ν_{asym})	3366	ν_{asym} NH ₂ of Cytosine + ν_3 of NH ₃ (ν_{asym})	3373	ν_3 of NH ₃ (ν_{asym})
3259	ν_3 of H ₂ O (ν_{asym})	3268	ν_3 of H ₂ O (ν_{asym})	3270	ν_3 of H ₂ O (ν_{asym})
2948	ν C-H; ν N-H of Uracil	3172	ν_{sym} NH ₂ of Cytosine	2970	ν CH ₃ of Thymine
2867	ν C-H; ν N-H of Uracil	2959	ν_9 of CH ₃ OH (ν_{asym} CH ₃)	2918	ν CH ₃ of Thymine
2828	ν_3 of CH ₃ OH (ν_{sym} CH ₃)	2828	ν_3 of CH ₃ OH (ν_{sym} CH ₃)	2829	ν_3 of CH ₃ OH (ν_{sym} CH ₃)
2136	1-0 mode of CO (ν)	2136	1-0 mode of CO (ν)	2137	1-0 mode of CO (ν)
1737	ν C=O of Uracil	1661	ν C=O of Cytosine + ν_2 of H ₂ O (β)	1689	ν C=C + ν_2 of H ₂ O (β)
1713	ν C=O of Uracil	1632	ν C=O of Cytosine + ν_2 of H ₂ O (β)	1674	ν C=C + ν_2 of H ₂ O (β)
1664	ν_2 of H ₂ O (β)	1616	ν C=C of Cytosine		
1644	ν C=C of Uracil + ν_2 of H ₂ O (β)	1540	β N-H of Cytosine	1460	β CH ₃ of Thymine + ν_4 and ν_{10} of CH ₃ OH (β CH ₃ and β OH)
1613	β C-H of Uracil	1515	ν C=N and ν C-N of Cytosine	1427	β CH ₃ of Thymine
1461	ν Ring, ν C-N and β N-H of Uracil + ν_4 and ν_{10} of CH ₃ OH (β CH ₃ and β OH)	1467	ν C-N of Cytosine + ν_4 and ν_{10} of CH ₃ OH (β CH ₃ and β OH)	1249	ν Ring of Thymine
1423	ν C-N and β N-H of Uracil	1367	β C-H of Cytosine	1212	β C-H, ν C-N, ν C-C, ν CH ₃ of Thymine
1395	β N-H; β C-H and ν C-N of Uracil	1281	ν C-N of Cytosine	1126	ν_2 of NH ₃ (umbrella mode)
1240	ν Ring of Uracil	1236	ν C=O of Cytosine	1026	ν_8 of CH ₃ OH (ν CO)
1124	ν_2 of NH ₃ (umbrella mode)	1161	ν_2 of NH ₃ (umbrella mode)	939	ν C-N of Thymine
1025	ν_8 of CH ₃ OH (ν CO)	1126	ν_8 of CH ₃ OH (ν CO)	847	γ N-H of Thymine
886	γ N-H of Uracil	1024	γ NH ₂ of Cytosine	816	Ring breathing and γ C=O of Thymine
760	Ring breathing of Uracil	834	γ C=O of Cytosine		
		796	γ C=O of Cytosine		
		785	γ C=O of Cytosine		
		764	Ring breathing of Cytosine		
		705	β Ring of Cytosine		

Note. ^aBouilloud et al. (2015).

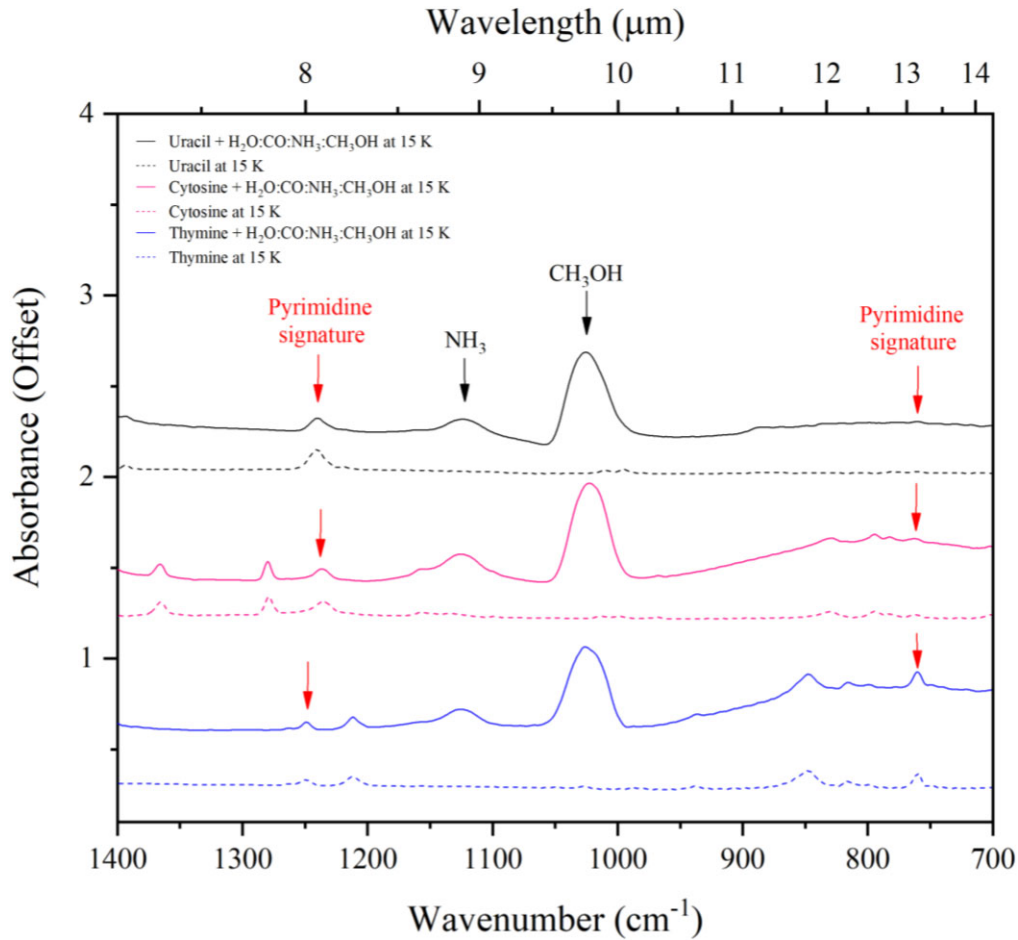


Figure 5. The mid-IR spectra of uracil (upper line), cytosine (middle line), and thymine (bottom line) in the region where are found common bands of pyrimidines ($1400\text{--}700\text{ cm}^{-1}$). The red (light) arrows indicate the two pyrimidines bands that are not covered by the ice mixture containing $\text{H}_2\text{O}:\text{CO}:\text{NH}_3:\text{CH}_3\text{OH}$. The bands of interest are: 1242 ± 6 and $761 \pm 2\text{ cm}^{-1}$.

Table 3. Characterization of IR bands for uracil, thymine, and cytosine within interstellar ices.

$\nu(\text{cm}^{-1})$	$\lambda (\mu\text{m})$	Assignment	ψ (km/mol)
1242 ± 6	8.05 ± 0.08	ν Ring of uracil and thymine + ν C-N of cytosine	47 (U); 14 (T); 19 (C)
761 ± 2	13.14 ± 0.10	Ring breathing of uracil, thymine, and cytosine	8.7 (T);

Note. ^aIglesias-Groth & Cataldo (2023).

ing); Writing – review and editing (supporting). Marcelo Emilio: Conceptualization (supporting); Writing – original draft (supporting); Writing – review and editing (supporting). Laerte Andrade: Conceptualization (supporting); Writing – original draft (supporting); Writing – review and editing (supporting). Eduardo Janot-Pacheco: Conceptualization (supporting); Writing – original draft (supporting); Writing – review and editing (supporting). Nigel Mason: Conceptualization (supporting); Writing – original draft (supporting); Writing – review and editing (supporting). Claudia Lage: Conceptualization (supporting); Formal analysis (supporting); Methodology (supporting); Supervision (equal); Writing – original draft (supporting); Writing – review and editing (supporting).

ACKNOWLEDGEMENTS

We thank Sao Paulo Research Foundation (FAPESP) support through grant 2016/13750–6 and the Coordenação de Aperfeiçoamento de

Pessoal de Nível Superior – Brazil (CAPES) – Finance Code 001. LA thank to support with resources from Conselho Nacional de Pesquisa (CNPq) 300927/2023–1, and CAR and AB thank the Conselho Nacional de Desenvolvimento Científico e Tecnológico (CNPq) for support through grants 401567/2022–2 and 309258/2023–5. AB thank the Instituto Serrapilheira Serra-1912–31843. NJM recognizes support from the Europlanet 2024 RI which has been funded by the European Union’s Horizon 2020 Research Innovation Programme under grant agreement no. 87114 A. ME gratefully acknowledges the financial support of the ‘Fenômenos Extremos do Universo’ of the Fundação Araucária.

DATA AVAILABILITY

The data underlying this article will be shared on reasonable request to the corresponding author.

REFERENCES

- Baek G., Lee J.-E., Hirota T., Kim K.-T., Kim M. K., 2022, *ApJ*, 939, 84
- Bergantini A., Abplanalp M. J., Pokhilko P., Krylov A. I., Shingledecker C. N., Herbst E., Kaiser R. I. 2018a, *ApJ*, 860, 108
- Bergantini A., Góbi S., Abplanalp M. J., Kaiser R. I., 2018b, *ApJ*, 852, 70
- Bergantini A., Maksyutenko P., Kaiser R. I., 2017, *ApJ*, 841, 96
- Boogert A. A., Gerakines P. A., Whittet D. C., 2015, *ARA&A*, 53, 541
- Boss A. P., 1998, *Annu. Rev. Earth Planet. Sci.*, 26, 53
- Bouilloud M., Fray N., Bénilan Y., Cottin H., Gazeau M.-C., Jolly A., 2015, *MNRAS*, 451, 2145
- Brünken S., McCarthy M., Thaddeus P., Godfrey P. D., Brown R., 2006, *A&A*, 459, 317
- Burton A. S., Stern J. C., Elsila J. E., Glavin D. P., Dworkin J. P., 2012, *Chem. Soc. Rev.*, 41, 5459
- Callahan M. P., Smith K. E., Cleaves H. J., Ruzicka J., Stern J. C., Glavin D. P., House C. H., Dworkin J. P., 2011, *Proc. Natl. Acad. Sci. USA*, 108, 13995
- Charnley S. B. et al., 2005, *Adv. Space Res.*, 36, 137
- Choughuley A., Subbaraman A., Kazi Z., Chadha M., 1977, *Biosystems*, 9, 73
- Chyba C., Sagan C., 1992, *Nature*, 355, 125
- Colarusso P., Zhang K., Guo B., Bernath P. F., 1997, *Chem. Phys. Lett.*, 269, 39
- Cooper G., Kimmich N., Belisle W., Sarinana J., Brabham K., Garrel L., 2001, *Nature*, 414, 879
- Cooper G., Rios A. C., 2016, *Proc. Natl. Acad. Sci. USA*, 113, E3322
- Coutens A., Loison J.-C., Boulanger A., Caux E., Müller H., Wakelam V., Manigand S., Jørgensen J., 2022, *A&A*, 660, L6
- Danger G., Bossa J.-B., De Marcellus P., Borget F., Duvernay F., Theulé P., Chiavassa T., d'Hendecourt L., 2011, *A&A*, 525, A30
- Deamer D. W., Pashley R., 1989, *Origins Life Evol. Biospheres*, 19, 21
- Dullemont C., Isella A., Andrews S., Skobleva I., Dzyurkevich N., 2020, *A&A*, 633, A137
- Ferris J. P., Sanchez R. A., Orgel L. E., 1968, *J. Mol. Biol.*, 33, 693
- Fornaro T., Biczysko M., Monti S., Barone V., 2014, *Phys. Chem. Chem. Phys.*, 16, 10112
- Fox S. W., Harada K., 1961, *Science*, 133, 1923
- Furukawa Y., Chikaraishi Y., Ohkouchi N., Ogawa N. O., Glavin D. P., Dworkin J. P., Abe C., Nakamura T., 2019, *Proc. Natl. Acad. Sci. USA*, 116, 24440
- Gibb E., Whittet D., Boogert A., Tielens A., 2004, *ApJS*, 151, 35
- Guélin M., Cernicharo J., 2022, *Front. Astron. Space Sci.*, 9, 787567
- Hayatsu R., Studier M. H., Moore L. P., Anders E., 1975, *Geochim. Cosmochim. Acta*, 39, 471
- Herbst E., Van Dishoeck E. F., 2009, *ARA&A*, 47, 427
- Iglesias-Groth S., Cataldo F., 2023, *MNRAS*, 523, 1756
- Ioppolo S. et al. 2021, *Nat. Astron.*, 5, 197
- Janot-Pacheco E., Rachid M., Bendjoya P., Domiciano A., Antunes-Rosa C., Emilio M., Lage C., 2018, in *Proc. IAU Symp. 345, Origins: From the Protosun to the First Steps of Life*. Kluwer, Dordrecht, p. 215
- Kitadai N., Maruyama S., 2018, *Geosci. Front.*, 9, 1117
- Kobayashi K., 2019, *Astrobiology*. Springer, Berlin, p. 43
- Kuan Y.-J., Charnley S. B., Huang H.-C., Kisiel Z., Ehrenfreund P., Tseng W.-L., Yan C.-H., 2004, *Adv. Space Res.*, 33, 31
- Kwiatkowski J. S., Leszczyński J., 1996, *J. Phys. Chem.*, 100, 941
- Leś A., Adamowicz L., Nowak M. J., Lapinski L., 1992, *Spectrochim. Acta A*, 48, 1385
- Maity S., Kaiser R. I., Jones B. M., 2015, *Phys. Chem. Chem. Phys.*, 17, 3081
- Martins Z. et al., 2008, *Origins Life Evol. Biospheres*, 30, 214
- Materese C. K., Nuevo M., Bera P. P., Lee T. J., Sandford S. A., 2013, *Astrobiology*, 13, 948
- Materese C. K., Nuevo M., McDowell B. L., Buffo C. E., Sandford S. A., 2018, *ApJ*, 864, 44
- Materese C. K., Nuevo M., Sandford S. A., 2017, *Astrobiology*, 17, 761
- Mathlouthi M., Seuvre A. M., Koenig J. L., 1986, *Carbohydr. Res.*, 146, 1
- McClure M. K. et al., 2023, *Nat. Astron.*, 7, 431
- Mejía C. et al., 2023, *Nucl. Instrum. Methods. Phys. Res. B.*, 534, 11
- Nowak M., Lapinski L., Fulara J., 1989, *Spectrochim. Acta A*, 45, 229
- Nuevo M., Milam S. N., Sandford S. A., 2012, *Astrobiology*, 12, 295
- Nuevo M., Milam S. N., Sandford S. A., Elsila J. E., Dworkin J. P., 2009, *Astrobiology*, 9, 683
- Nuevo M., Sandford S. A., 2014, *ApJ*, 793, 125
- Oba Y., Takano Y., Furukawa Y., Koga T., Glavin D. P., Dworkin J. P., Naraoka H., 2022, *Nat. Commun.*, 13, 2008
- Oba Y., Takano Y., Naraoka H., Watanabe N., Kouchi A., 2019, *Nat. Commun.*, 10, 1
- Öberg K. I., 2016, *Chem. Rev.*, 116, 9631
- Öberg K. I., Boogert A. A., Pontoppidan K. M., Van den Broek S., Van Dishoeck E. F., Bottinelli S., Blake G. A., Evans I. I. N. J., 2011, *ApJ*, 740, 109
- Parker D. S., Kaiser R. I., Kostko O., Troy T. P., Ahmed M., Mebel A. M., Tielens A. G., 2015, *ApJ*, 803, 53
- Radchenko E., Sheina G., Smorygo N., Blagoi Y. P., 1984, *J. Mol. Struct.*, 116, 387
- Rocha W. R. M. et al., 2024, *A&A*, 683, A124
- Rosa C. A. et al., 2023, *Life*, 13, 2208
- Rubin R. H., Swenson G. W., Jr, Benson R. C., Tigelaar H. L., Flygare W. H., 1971, *ApJ*, 169, L39
- Ruf A., Lange J., Eddhif B., Geffroy C., Hendecourt L. L. S., Poinot P., Danger G., 2019, *ApJ*, 887, L31
- Saiagh K., Cloix M., Fray N., Cottin H., 2014, *Planet. Space Sci.*, 90, 90
- Saiagh K., Cottin H., Aleian A., Fray N., 2015, *Astrobiology*, 15, 268
- Saladino R., Ciambecchini U., Crestini C., Costanzo G., Negri R., Di M. E., 2003, *ChemBioChem*, 4, 514
- Saladino R., Crestini C., Ciambecchini U., Ciciriello F., Costanzo G., Di M. E., 2004, *ChemBioChem*, 5, 1558
- Saladino R., Crestini C., Costanzo G., Negri R., Di M. E., 2001, *Bioorg. Med. Chem.*, 9, 1249
- Saladino R., Crestini C., Neri V., Brucato J. R., Colangeli L., Ciciriello F., Di M. E., Costanzo G., 2005, *ChemBioChem*, 6, 1368
- Saladino R., Crestini C., Neri V., Ciciriello F., Costanzo G., Di M. E., 2006, *ChemBioChem*, 7, 1707
- Saladino R., Crestini C., Pino S., Costanzo G., Di M. E., 2012, *Phys. Life Rev.*, 9, 84
- Sandford S. A., Nuevo M., Bera P. P., Lee T. J., 2020, *Chem. Rev.*, 120, 4616
- Schwartz A. W., Chittenden G., 1977, *Biosystems*, 9, 87
- Sephton M. A., 2002, *Nat. Prod. Rep.*, 19, 292
- Shock E. L., Schulte M. D., 1990, *Geochim. Cosmochim. Acta*, 54, 3159
- Simon M. N., Simon M., 1973, *ApJ*, 184, 757
- Singh J., 2008, *J. Mol. Struct.*, 876, 127
- Stoks P. G., Schwartz A. W., 1979, *Nature*, 282, 709
- Susi H., Ard J. S., 1971, *Spectrochim. Acta A*, 27, 1549
- Szczepaniak K., Szczesniak M. M., Person W. B., 2000, *J. Phys. Chem. A*, 104, 3852
- Szczesniak M., Nowak M., Szczepaniak K. et al., 1985, *Spectrochim. Acta A*, 41, 237
- Szczesniak M., Szczepaniak K., Kwiatkowski J., KuBulat K., Person W., 1988, *J. Am. Chem. Soc.*, 110, 8319
- Turner B. E., 1971, *ApJ*, 163, L35
- Vasyunin A. I., Caselli P., Dulieu F., Jiménez-Serra I. 2017, *ApJ*, 842, 33
- Vignoli Muniz G. S., Agnihotri A. N., Augé B., Mejía C., Martínez R., Rothard H., Domaracka A., Boduch P., 2022, *ACS Earth Space Chem.*, 6, 2149
- Zhang Z. E., Yang Y.-l., Zhang Y., Cox E. G., Zeng S., Murillo N. M., Ohashi S., Sakai N., 2023, *ApJ*, 946, 113

This paper has been typeset from a $\text{\TeX}/\text{\LaTeX}$ file prepared by the author.